IEEE Access
Multidisciplinary | Rapid Review | Open Access Journal

Received April 19, 2019, accepted May 17, 2019, date of publication May 23, 2019, date of current version June 6, 2019.

Digital Object Identifier 10.1109/ACCESS.2019.2918559

Gait Event Anomaly Detection and Correction During a Split-Belt Treadmill Task

USMAN RASHID[1], NITIKA KUMARI[1], DENISE TAYLOR[1], TIM DAVID[2], AND NADA SIGNAL[1]
[1]Health and Rehabilitation Research Institute, Auckland University of Technology, Auckland 0627, New Zealand
[2]Department of Mechanical Engineering, University of Canterbury, Christchurch 8041, New Zealand

Corresponding author: Usman Rashid (urashid@aut.ac.nz)

ABSTRACT During instrumented split-belt treadmill tasks, it is challenging to avoid partially stepping on the contralateral belt. If this occurs, accurate detection of gait events from force sensors becomes impossible, as the force data are invalidated. In this paper, we present an algorithm, which automatically detects these invalid force data using an acceleration derivative-based measure. We used this algorithm in combination with the coordinate-based treadmill algorithm to replace the invalidated gait events detected from force sensors with those detected from 3-D markers. The performance of the proposed algorithm was evaluated against the visual examination of data collected from healthy participants in both the same speed and differential speed configurations, using the receiver operator characteristics, the area under the curve, and the Youden index. We found that the area under the curve (AUC) score was above 0.8 in both the same speed and differential speed configurations. Moreover, there was not enough evidence ($p > 0.05$) to suggest a correlation between walking speed and the performance of the algorithm. We conclude that the algorithm has good to excellent detection and correction performance, which can be useful for research involving analysis of gait with instrumented split-belt treadmills. A MATLAB (MathWorks, Inc., Natick, MA, USA) based implementation of the proposed algorithm and example data files are also presented.

INDEX TERMS Gait analysis, split-belt treadmill, anomaly detection, force plates, 3-D kinematics, accelerometers.

I. INTRODUCTION

A split-belt treadmill is a special type of treadmill which has a separate belt for each leg [1]. As both the belts are separate and individually actuated, the split-belt can be used in two speed configurations. (i) Same speed configuration (SS) in which both the belts move at the same speed. (ii) Differential speed configuration (DS) in which the two belts move at different speeds [2]. Split-belt walking, where one leg is forced to move at a faster speed, is a well studied task in humans, animals and using robots [3]–[14]. It is used in the study of locomotor learning in healthy and pathological populations as it provides a novel and perturbing locomotor environment [15]–[18]. Using split-belt treadmill researchers have also proposed a variety of gait rehabilitation paradigms for patients with motor impairments [19]–[21].

Force plates embedded in the belts, 3-D motion capture camera system, accelerometers, and gyroscopes are generally used to record different aspects of the gait during split-belt treadmill tasks [22]–[28]. Detection of heel-strike (HS) and toe-off (TO) at correct time points from the data recorded with these sensors play an importance role in gait analysis. These events determine the stance and swing phases of gait. Although gait events can be determined from a range of different sensors [29], the detection of gait events by setting a threshold for data obtained from force plates is generally considered the gold standard method [24], [30], [31]. For example, using a threshold of 20 Newtons, a HS is registered at the time when the increasing value of force crosses this threshold. Similarly a TO is registered at the time when the decreasing force crosses this threshold.

A. PROBLEM STATEMENT

Walking on the split-belt treadmill requires a wider base of gait [32] to ensure that the feet remain on the right and left belts respectively [33]. Failure to do so invalidates the force sensor data [34]. This becomes more evident when one has to

The associate editor coordinating the review of this manuscript and approving it for publication was Bora Onat.

walk for a longer duration such as 10–15 minutes. Placing a separator between the two belts is often recommended to avoid the crossing over of the feet [33], however this compromises the natural walking pattern. When thresholding method is used to detect gait events from the force data, it can lead to invalid events. One solution for this problem is to not use the force data and instead rely on secondary sensors such as 3-D kinematic data or accelerometers, however, this is known to be less accurate [35]. Another solution is to manually identify time intervals where force data is invalidated and switch back and forth between events from force plate and the secondary sensor. However, this solution becomes impracticable when analyzing a large dataset, such as a large number of participants, long session duration or multiple data collection sessions. Thus there is a need for a method which can automate the process of gait event detection from force plate data, identify invalidated force data due to placement of both feet on the same belt and correct for these invalidated force data.

B. PROPOSED SOLUTION

In this study we propose a detection and correction algorithm (DACA) which automatically marks time instances where the force data has been invalidated and replaces gait events in these instances with events derived from 3D markers. The proposed method uses an acceleration derivative based measure to transform force plate data into noise levels. It then uses adaptive statistical profiling to detect time intervals where force data has been invalidated due to placement of both feet on the same belt. Combined with existing methods of gait event detection from force plate data and 3-D motion capture system, the proposed method is capable of fully automated gait event detection and correction. The performance of the proposed algorithm was evaluated by comparing its performance against visual examination in both the same speed and differential speed configurations. To the best of our knowledge, this is the first solution for gait event detection and correction from force plates embedded in a split-belt treadmill.

II. METHODS

A. EXPERIMENTAL DATASET

The dataset used for evaluation of the proposed algorithm was taken from a randomized controlled trial involving walking on an instrumented split-belt treadmill (Bertec Corporation, Columbus, OH, USA). The sampling rate of the force platform was 1000 Hz. A nine-camera motion capture system (Vicon Vantage, Nexus 2.4, Vicon Motion Systems Ltd, Oxford, UK) was used to record position data at a frame rate of 200 Hz from 33 reflective markers placed according to the Cleveland clinic model [36]. An illustration of the split-belt treadmill used in this study is shown in Figure 1.

The trial investigated the effect of cerebellar transcranial direct current stimulation (ctDCS) on motor adaptation in a healthy population. Thirty participants (Average age: 30 ± SD 6 years, 12 female) were recruited through professional networks and local advertising. Participants were excluded if they had a history of orthopaedic, cardiac or neurological conditions that could interfere with walking, or any contra-indications to application of ctDCS. All the participants provided written consent before data collection. Ethics approval (16/338) for the study was obtained from Auckland University of Technology Ethics Committee. Data was collected over four $1\frac{1}{2}$ hour sessions at the Running and Cycling Clinic, AUT Millennium Institute, New Zealand.

FIGURE 1. An illustration of the split-belt treadmill used in this study.

Whilst walking on the treadmill, participants were instructed to look straight ahead and stay in the middle of the treadmill with one foot on each belt, and holding a front rail adjusted to their elbow height. The participant's fastest comfortable walking speed on the treadmill was determined. During data collection the participants walked for a total of 25 minutes where 15 minutes were undertaken with the belts moving at different speeds followed by 10 minutes with both belts moving at same speeds. In the differential speed configuration the fast belt speed was set to the participant's fastest comfortable waking speed and the slow belt to half of this speed. The treadmill was configured such that the fast belt was under the participant's dominant leg. In the same speed configuration both belts were set to half of the participant's fastest comfortable walking speed.

To evaluate the proposed algorithm, the six data files with the highest prevalence of invalid force data were selected from each speed configuration. These files included data from 6 different participants over four different sessions. The fastest comfortable walking speed for these participants ranged from 1.1 to 2.1 meters/second (m/s).

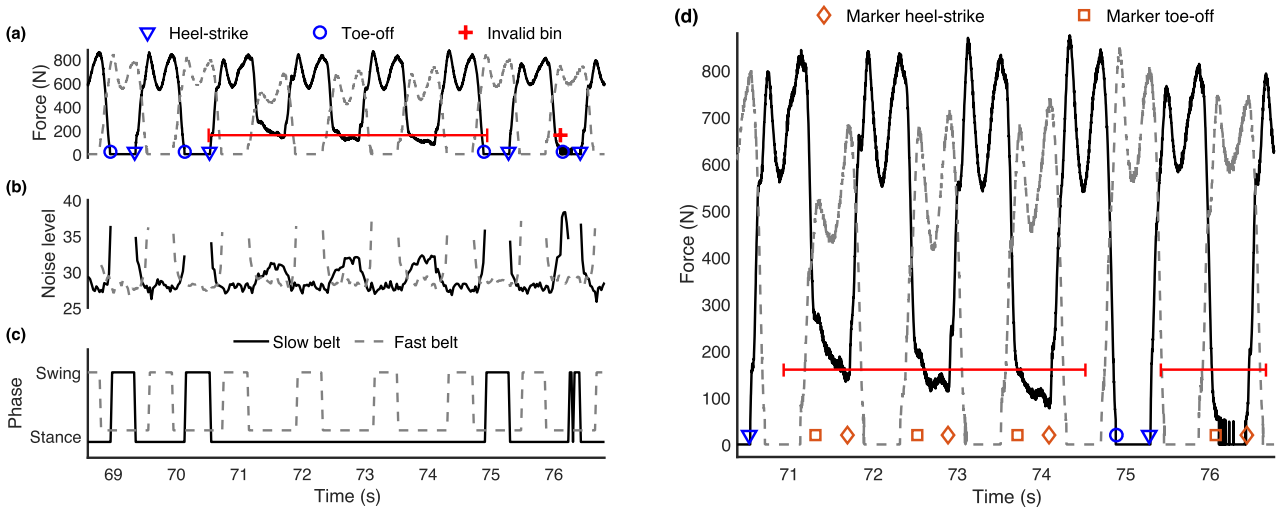

FIGURE 2. Detection and correction of gait events where the force data is invalid. '⊢⊣' represents intervals of invalid force.

B. EVENT DETECTION FROM FORCE PLATES

To determine heel-strikes and toe-offs for each foot, the data from force plates was first filtered with a 2^{nd} order zero-phase low-pass Butterworth filter with cut-off at 10 Hz. The filtered force was used to obtain the heel-strikes and toe-offs with a threshold at 20 Newtons. A HS was registered at the time when the increasing value of force crossed this threshold. Similarly a TO was registered at the time when the decreasing force crossed this threshold. These events are shown in Figure 2 (a). Mathematically, it was achieved by applying the first order difference operation to the threshold data. The time of positive differences were marked as heel-strikes and time of negative differences as toe-offs.

C. DETECTION AND CORRECTION ALGORITHM (DACA)

The time points and intervals where the force plate data was invalidated by placement of both feet on the same plate were detected by transforming the raw force values to noise levels. This was done by binning raw force data into bins of length 25 milliseconds and finding noise level in each bin. The bin length was chosen to strike a balance between computation time required for data processing and capturing faster dynamics of force data. The noise level was defined as the natural log of the integral of the square of the acceleration derivative as given below.

$$n_i(x) = \ln\left|\frac{1}{(x_i^{peak})^2}\int_{t_i}^{t_{i+1}}\left(\frac{d^3}{dt^3}x(t)\right)^2 dt\right| \tag{1}$$

where $x(t)$ is the raw force plate data, and x_i^{peak}, $n_i(x)$ define the peak raw force value and the measure of noise for the i^{th} bin respectively. This noise measure is similar to the log dimensionless acceleration derivative used to quantify movement smoothness [37]. The noise levels for the bins are shown in Figure 2 (b). Assuming that the raw force data was divided into k bins, the mean and standard deviation of the noise levels from these bins were defined as follows.

$$\bar{n} = \frac{\sum_{i=1}^{k} n_i}{k}$$
$$\sigma_n = \sqrt{\frac{\sum_{i=1}^{k}(n_i - \bar{n})^2}{k-1}} \tag{2}$$

If k_b number of consecutive bins had a noise level above the mean ($\bar{n}$) plus one standard deviation (σ_n), the first bin was marked invalid as shown by '+' in Figure 2 (a). The number of bins (k_b) was used to select the sensitivity of the detector to invalid force.

In reference to the slow belt force data in Figure 2 (a), as the foot was lifted completely off the belt at toe-off, the force became zero. The force remained zero during a normal swing phase and started increasing again at the heel-strike. However in case of the third, fourth and the fifth swing phase, the force did not become zero as the contralateral foot was partially placed on the slow belt. This non-zero force during a swing phase signified the crossing over of feet across belts. When the force was zero, the noise level in corresponding bins was *undefined* as x_i^{peak} was zero. This can be observed in Figure 2 (b), where the plotted noise levels have gaps. These periods of *undefined* noise level correspond to swing phase and the periods of *defined* noise level correspond to the stance phase, as shown in Figure 2 (c). This definition of swing and stance phase gives poor estimates of the actual phases because the accuracy of the estimates is dependent on bin size. However the advantage is that the obtained values do not depend on detected force events. The mode statistic of the time duration of these stance phases was defined as the mode stance time and it was used to identify invalid force intervals. Thus a stance phase which was longer than twice the mode stance time was identified as an invalid force interval, under the assumption that such a stance phase is not

naturally possible. The resulting intervals of invalid force are represented by '⊢⊣' in Figure 2 (a, d).

These intervals and bins of the detected invalid force were then used to remove gait events detected from force data and were replaced by events detected from 3-D marker data. This process of detection and replacement of anomalous gait events was done for each belt separately. The results are shown in Figure 2 (d).

The detected bins of invalid force could not be directly used to remove and replace nearby invalid gait events as the bin size (25 milliseconds) was too short. Thus an interval was created at the time of the invalid bin time. The length of these intervals in each direction was set to three quarters of the mode stance time. This length was chosen to ensure that the nearby invalid events were removed and replaced while valid events from adjacent phases were not. The use of mode stance time for this purpose also ensured that this operation was adaptive to speed changes across belts and participants. The lengths of the detected intervals of invalid force were shortened in each direction by half of the mode stance time. This was done to avoid unnecessarily removing valid force events from adjacent phases.

D. EVENT DETECTION FROM 3-D MARKER DATA

To detect gait events from the 3-D marker data, a modified form of the Coordinate-based Treadmill Algorithm was used [38]. First the marker data was low pass filtered using a 2^{nd} order zero-phase Butterworth filter with cut-off at 25 Hz. The zero-phase filter does not introduce a time lag in the signal and, therefore, does not disrupt the time synchronization between the force plate data and 3-D marker data. Second, the heel-strikes for the left and the right foot were detected as the maxima of the left and the right heel marker position in the anterior-posterior direction respectively. Similarly the toe-offs for the left and the right foot were detected as the minima of the left and the right fifth metatarsal marker position in the anterior-posterior direction respectively.

E. VISUAL EXAMINATION OF DATA

The detection and correction performance of the algorithm was validated by comparison with detection and correction done by a trained examiner. A graphical tool was developed in MATLAB (MathWorks, Inc., Natick, MA, USA) 2017b for this purpose. The examiner inspected the raw force data of a single file at a time by scrolling through it in 10 second windows. The examiner marked an interval of invalid force by selecting a start and an end point. The gait events detected from both the force and the marker data in that interval were then revealed. The examiner reviewed each gait event and selected one of the estimates (force or marker event) and deleted the other.

F. STATISTICAL ANALYSIS

The statistical analysis was performed separately for the two speed configurations, the belt sides (the fast or dominant leg (DL) and the slow or non-dominant leg (NDL)), and excluded force, included marker events. This was done to consider the performance of the algorithm under varying conditions. To illustrate the scope of the problem, the prevalence of excluded force events was defined as the percentage of force events excluded by the examiner from the total number of force events detected. The prevalence of included marker events was defined as the percentage of markers events included by the examiner from the total detected marker events.

To evaluate the performance of the proposed algorithm, we compared; (a) whether the algorithm removed the same set of force events as the examiner and (b) whether the algorithm included same marker events as the examiner. These assessments were made using receiver operator characteristic curves (ROC). It is a graphical tool for visualizing the performance of classifiers [39]. It shows the performance of a classifier in terms of the trade-off between its true positive rate (TRP, hit rate, sensitivity) and its false positive rate (FPR, fall-out). For comparison with the random performance, an identity line (TPR = FPR) is also plotted. The farther is the ROC curve of a classifier above the random performance line, the better is its classification ability. In order to assess the ability of the proposed method to both exclude invalidated force events and include valid marker events, we plotted separate ROC curves. Also separate ROC curves were plotted for the slow belt and the fast belt in the two speed configurations. Thus a total of 8 ROC curves were plotted. All the 6 data files of each speed configuration were used in plotting a curve. To plot a curve we computed TRP and FPR as a function of the number of bins (k_b) used by the proposed algorithm. Its value was varied from 1 to 10. For each value of k_b we computed TPR and FPR for the six data files and averaged TPR and FPR across these files. This corresponded to the threshold averaging method explained by Fawcett [39]. True positive rate for excluded force events (TPR_f), false positive rate for excluded force events (FPR_f), true positive rate for included marker events (TPR_m) and false positive rate for included marker events (FPR_m) was defined as follows.

$$TPR_f = \frac{TP_f}{P_f} \times 100 \tag{3}$$

$$FPR_f = \frac{FP_f}{N_f} \times 100 \tag{4}$$

$$TPR_m = \frac{TP_m}{P_m} \times 100 \tag{5}$$

$$FPR_m = \frac{FP_m}{N_m} \times 100 \tag{6}$$

TP_f True positive force events: Force events excluded by both the algorithm and the examiner.

FP_f False positive force events: Force events excluded by the algorithm and not by the examiner.

P_f Positive force events: Force events excluded by the examiner.

N_f Negative force events: Force events not excluded by the examiner.

TABLE 1. Means and standard deviations for prevalence of excluded force events and included marker events. NDL stands for non-dominant leg. DL stands for dominant leg. The differential speed configuration corresponds to both the belts moving at different speed with a ratio of 1:2. The same speed configuration corresponds to both the belt moving at same speed with a ratio of 1:1.

Events	Speed configuration	Slow belt (NDL) (%)	Fast belt (DL) (%)
Excluded force	Differential	3.67 ± 2.67	0.18 ± 0.15
	Same	9.45 ± 5.48	0.39 ± 0.72
Included marker	Differential	3.67 ± 2.444	0.23 ± 0.25
	Same	18.05 ± 8.81	0.53 ± 0.95

TP_m True positive marker events: Marker events included by both the algorithm and the examiner.

FP_m False positive marker events: Marker events included by the algorithm and not by the examiner.

P_m Positive marker events: Marker events included by the examiner.

N_m Negative marker events: Marker events not included by the examiner.

To represent ROC performance as a scalar value, we obtained area under the curve (AUC). The AUC score was interpreted as the probability that the proposed algorithm correctly labeled a randomly chosen positive case against a randomly chosen negative case. Thus an AUC score of 1.0 was considered perfect discriminative ability and 0.5 represented random guessing [39]. To identify optimal number of bins (k_b), we obtained Youden index [40]. It was computed as TPR – FPR at each point of the ROC curve and its maximum value (YI_{max}) corresponded to the optimal number of bins (k_b). YI_{max} was interpreted as informedness of the proposed method with 1.0 considered perfect discriminative ability and 0 as random guessing.

To evaluate the relationship between the walking speed of participants and the performance of the proposed method, the Spearman's rank correlation coefficient (ρ) and p-value for zero correlation null hypothesis (H_0: $\rho = 0$) was obtained. The correlation was performed between speed and true positive rate, speed and false positive rate. Significance level was set at 0.05. True positive rates and false positive rates were obtained for excluded force events and included marker events for each belt in each speed configuration as explained in Equations 3 – 6. To keep the analysis simple, no distinction was made between belts, speed configuration, excluded force events or included marker events while performing the correlation. Nonetheless a different number of bins (k_b) parameter of the algorithm was chosen for each speed configuration as dictated by the ROC analysis. Moreover, for the differential speed configuration, the fastest comfortable walking speed was treated as the walking speed. And for the same speed configuration, half of the fastest comfortable walking speed was treated as the walking speed.

Finally to show the implication of using the proposed algorithm on standard gait analyses, we compared the step lengths measured using the corrected gait events derived from DACA against the uncorrected gait events derived from force plates using the threshold method. The step length for both the DL and the NDL of one of the participants was obtained for this purpose. The step length for the DL was calculated for each step at heel-strike as the distance from the DL heel marker to the NDL heel marker. Similarly the step length for the NDL was calculated for each step at heel-strike as the distance from the NDL heel marker to the DL heel marker.

III. RESULTS

A. PREVALENCE

Table 1 lists the prevalence of excluded force events and included marker events by the examiner. The prevalence of included marker events was higher compared to the prevalence of excluded force events due to the fact that in many cases gait events were not detected at all from invalidated force data. The prevalence rates were higher in same speed configuration compared to the differential speed configuration. The rates were also higher for the slow belt compared to the fast belt. These results are further discussed later in Section IV.

B. RECEIVER OPERATOR CHARACTERISTICS

The receiver operator characteristic curves are given in Figure 3. With a single bin ($k_b = 1$) the true positive and the false positive rates for both the excluded force events and the included marker events were equal to 100%. As the number of bins were increased, the false positive rate decreased more rapidly than the true positive rate. This was also reflected by the area under the curve which was above 0.8 in all cases, refer to Table 2. The algorithm demonstrated good performance (AUC > 0.8) for slow belt (NDL) in the differential speed configuration and excellent performance (AUC > 0.9) in all other cases.

The number of bins corresponding to YI_{max} was 3 for both marker and force events for both the slow and the fast belt in the differential speed configuration. In the same speed configuration the number of bins corresponding to YI_{max} was 5 for both the belts for the force events. For the marker events, the number of bins was 6 for slow belt (NDL) and 5 for the fast belt (DL). These results indicated that the algorithm achieved consistent performance under same parameter value within a speed configuration.

C. RELATIONSHIP BETWEEN SPEED AND PERFORMANCE

True positive rates and false positive rates for excluded force events, included marker events, belts and speed

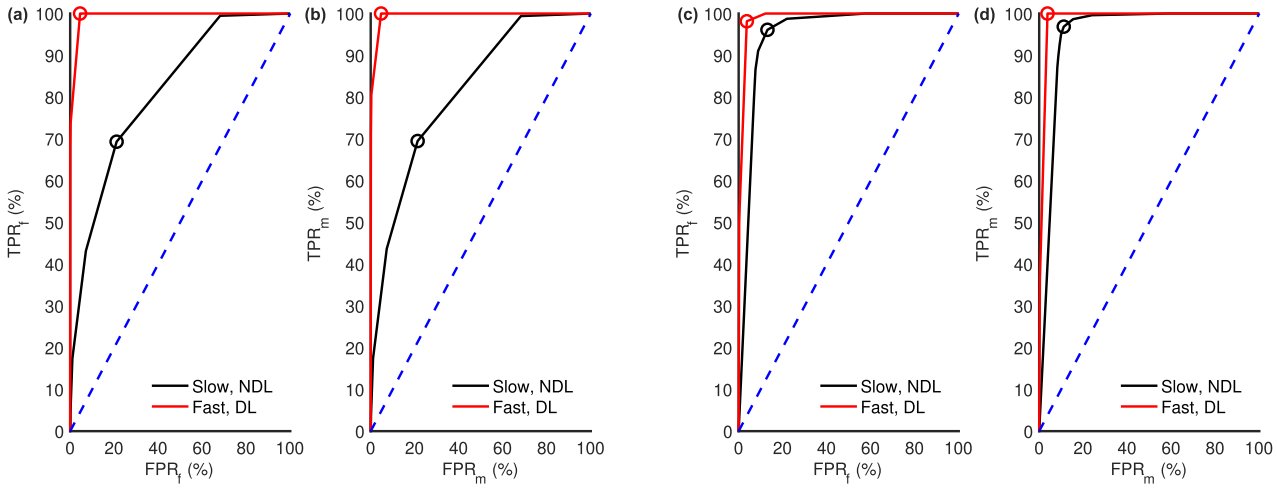

FIGURE 3. Differential speed (a, b) and same speed (c, d) configuration receiver operator characteristics curves for excluded force events and included marker events by the algorithm. 'o' represents the point corresponding to maximum Youden index. NDL stands for non-dominant leg. DL stands for dominant leg. TPR_f and FPR_f are the true positive and the false positive rates for the excluded force events respectively. TPR_m and FPR_m are the true positive and the false positive rates for the included marker events respectively.

TABLE 2. Performance metrics for the proposed algorithm under different conditions. NDL stands for non-dominant leg which was over the slow belt. DL stands for dominant leg which was over the faster belt. k_b represents the number of bins parameter of the algorithm. YI_{max} represents the maximum value of the Youden index.

Speed configuration	Events	Belt	Area under the curve	YI_{max}	k_b at YI_{max}
Differential	Excluded force	NDL	0.81	0.48	3
		DL	0.98	0.96	3
	Included marker	NDL	0.81	0.48	3
		DL	0.99	0.95	3
Same	Excluded force	NDL	0.94	0.83	5
		DL	0.99	0.94	5
	Included marker	NDL	0.95	0.86	6
		DL	0.99	0.96	5

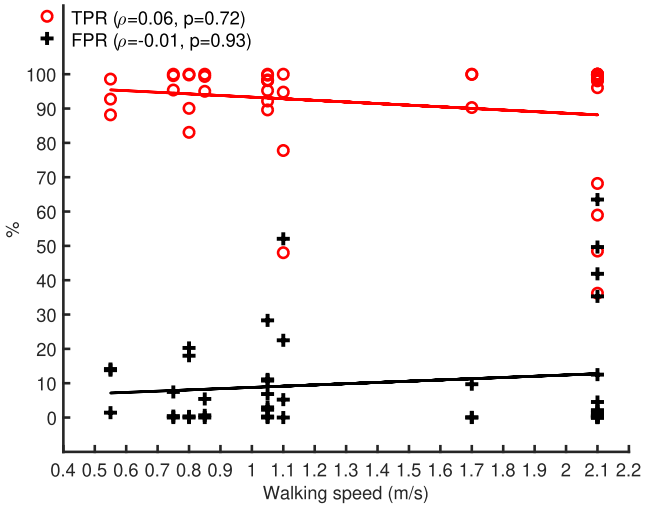

FIGURE 4. True positive rate (TPR) and false positive rate (FPR) plotted against walking speed. ρ, 'p' represent the Spearman's rank correlation coefficient and its corresponding p-value respectively. The solid lines represent the least-squares best fit lines.

configurations are plotted against the walking speed in Figure 4. As dictated by the results of the ROC analysis (Table 2), these TPRs and FPRs were obtained with number of bins (k_b) equal to 3 and 5 for the differential and the same speed configuration, respectively. The correlation between TRP and speed, FPR and speed was 0.06 and 0.01, respectively. There was not enough evidence ($p > 0.05$) to suggest a statistically significant correlation in either case. However there were a few large outliers which are discussed later in Section IV.

D. COMPARISON WITH FORCE THRESHOLD METHOD

Step lengths measured using uncorrected gait events derived with the force threshold method and gait events corrected using DACA are shown in Figure 5 (a) and (b) respectively. The uncorrected gait events resulted in a smaller number of steps (318) with multiple step length outliers. Whereas DACA corrected gait events identified a larger number of steps (352) and normally distributed step lengths.

IV. DISCUSSION

We have developed a novel algorithm which automatically detects invalid force data during a split-belt treadmill task. This rigorous evaluation of the performance of the algorithm indicates that it has good to excellent detection and correction performance in both the same speed and differential speed configurations.

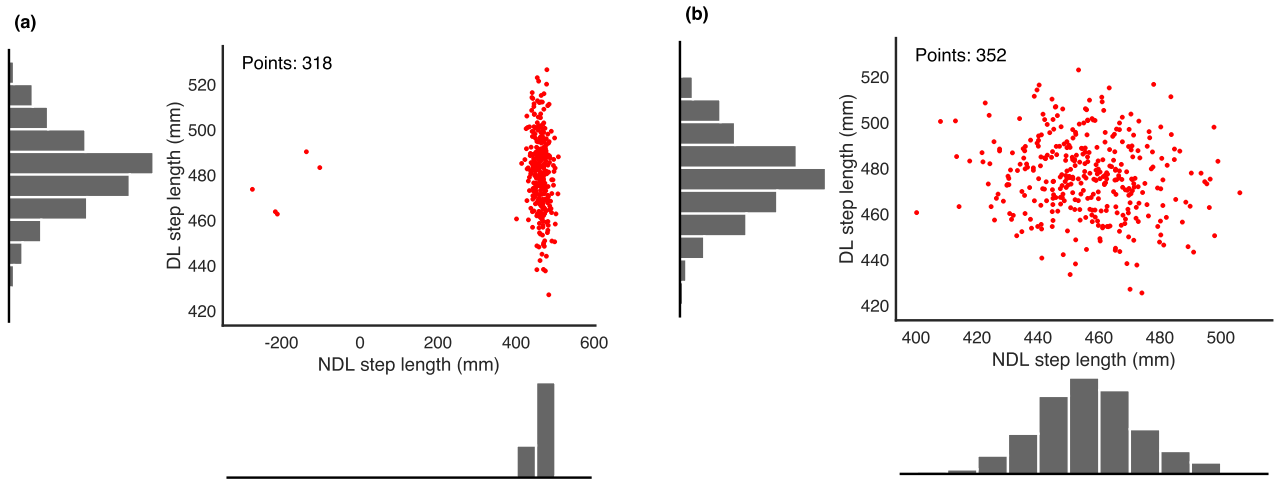

FIGURE 5. Step lengths for the dominant (DL) and the non-dominant leg (NDL) measured using uncorrected gait events derived with the force threshold method (a) and gait events corrected using the proposed method (b). The number of points correspond to the number of steps identified from the gait events.

The prevalence of invalidated and corrected gait events as determined by the examiner varied between 0.18% and 18% dependent upon the speed configuration and duration of the task, illustrating the scope of the problem. This has led researchers to use belt separators which changes the task [33], discard parts of the data or abandon the use of force data in favor of other sensors [34]. Thus the proposed method provides a viable alternative with the benefit of reduced processing time compared to manual examination and correction. Also it results in more robust events for gait analyses as compared to automatic event detection using the force plates alone.

The prevalence of both the excluded force events and included marker events was considerably higher for the slow belt in both differential speed and same speed configurations. The higher prevalence for the slow belt relates to the dominant leg stepping onto the slow belt. This suggests that prevalence of invalid force events is related to leg dominance and not to belt speed. The prevalence of included marker events was also higher compared to the prevalence of excluded force events due to the fact that in many cases, gait events were not detected at all from invalidated force data. Furthermore the prevalence was higher in same speed configuration. This may be due to familiarization to same speed configuration which has been found to narrow the base of gait over time [5], or fatigue resulting from 15 minutes of walking in the differential speed configuration which preceded the same speed configuration in this study.

The parameters of the algorithm are simple, intuitive and can be tuned manually. In future applications, the parameters can be fine tuned to meet the characteristics of the force sensor, the split-belt task and the population. All of the algorithm parameters, except for the length and number of bins, are based on the statistical properties of the recorded data and, thus, adaptive to differences in data. The length of the bin should be chosen based upon the sampling rate of the force sensor, rate of change of force dynamics, and the computational power required to process the data. The number of bins was used to select the sensitivity of the proposed algorithm. Its effect on the performance of the algorithm was studied using the ROC analysis. A larger number of bins reduced the sensitivity and a smaller number of bins increased the sensitivity of the algorithm. The analysis showed that the number of required bins differs across speed configurations, however the same number of bins produce consistent detection performance within the same configuration. This finding is important as only one bin number can be used for processing data for a given configuration. We recommend the use of 3 to 6 bins.

The walking speed of the participant on the split-belt treadmill did not have an effect on the performance of the algorithm in general. The significance of this result is amplified by the fact that same number of bins was used for all the data files for a given speed configuration. Thus, in future application, one can expect generally high detection and correction performance from the proposed algorithm without tuning its parameters for each data file. However as a few large outliers were observed in the speed versus performance analysis, fine tuning of parameters might be inevitable in some instances. A quick diagnostic tool to help this process is the scatter histogram plot of the outcome variable (e.g. step length) as shown in Figure 5. This plot gives a comprehensive overview of the performance of the algorithm and can be used to decide if the algorithm is performing well for the given data file with the selected parameters without the need to scroll through long raw force data. If there are outliers and the distribution of the outcome variable is not as expected, the parameters of the algorithm can be readjusted till desired performance is achieved.

Another important consideration for processing of force sensor data and 3-D marker data is the selection of the cut-off for the low pass filter. In the past, researchers have used varying cut-offs depending on the sensor characteristics, task and the population. For example, for force sensor data, cut-offs at 50 Hz and 20 Hz have been used [24], [38]. Whereas for 3-D marker data, cut-offs at 6 Hz, 7 Hz 10 Hz and 12 Hz were used [24], [25], [31], [41], [42]. In this study we used 10 Hz cut-off for force sensor data and 25 Hz cut-off for 3-D marker data. These cut-offs may compromise the performance of the proposed method in a different population or task. Therefore fine tuning of the cut-offs is suggested for future application in accordance with the sensor characteristics, the task and the population.

We used a 3D marker system to replace invalid gait events from force data or add gait events not detected altogether. Whilst we used the coordinate-based treadmill algorithm to detect gait events from 3D markers, the proposed algorithm can be used with any other algorithm which suits the needs of the researcher. Furthermore it can also be used in combination with an algorithm which detects gait events from other sensors such as accelerometers [26].

The findings of this research should be considered in light of a number of factors. The algorithm uses square of the acceleration derivative to transform the force values into noise levels. Force values with high noise level are labeled as invalid. Mean and standard deviation of the noise levels are used for this purpose. The algorithm also uses these noise levels to estimate swing and stance phases. Those stance phases which are longer than twice the time for most of the stance phases are also labeled as invalid using the mode statistic. Therefore the performance of the algorithm is expected to deteriorate under extremely high prevalence of invalid force where mean, standard deviation and mode can not adequately represent the data characteristics.

A. SOFTWARE AVAILABILITY

The MATLAB (MathWorks, Inc., Natick, MA, USA) based implementation of the proposed algorithm, the graphical user interface tool for visual examination and example data files have been made available online.[1] These tools can be used to import force plate and 3-D marker data from Vicon Nexus, process the data using the proposed algorithm and visualize the invalidated and corrected gait events.

V. CONCLUSION

We have proposed an algorithm which accurately detected invalidated force during an instrumented split-belt treadmill task due to placement of both feet on the same belt. Coupled with a secondary sensor, 3-D markers in this study, the proposed algorithm can automatically replace invalidated gait events in force data with gait events detected from the secondary sensor. ROC curve analysis on data collected from healthy participants in both the same speed and differential speed configurations showed that the proposed algorithm has good to excellent detection and correction capacity. Its performance was also robust to walking speed.

[1] https://github.com/GallVp/knkTools

ACKNOWLEDGEMENTS

The authors would like to thank Arun Kumar (CAITFS Lab, NSIT, Delhi University, India) for reviewing and proof reading the manuscript.

REFERENCES

[1] E. E. Helm and D. S. Reisman, "The split-belt walking paradigm: Exploring motor learning and spatiotemporal asymmetry poststroke," *Phys. Med. Rehabil. Clinics*, vol. 26, no. 4, pp. 703–713, 2015.
[2] H. Yokoyama, K. Sato, T. Ogawa, S.-I. Yamamoto, K. Nakazawa, and N. Kawashima, "Characteristics of the gait adaptation process due to split-belt treadmill walking under a wide range of right-left speed ratios in humans," *PLoS ONE*, vol. 13, no. 4, 2018, Art. no. e0194875.
[3] W. Hoogkamer, "Perception of gait asymmetry during split-belt walking," *Exerc. Sport Sci. Rev.*, vol. 45, no. 1, pp. 34–40, 2017.
[4] E. Thelen, B. D. Ulrich, and D. Niles, "Bilateral coordination in human infants: Stepping on a split-belt treadmill," *J. Exp. Psychol., Hum. Perception Perform.*, vol. 13, no. 3, p. 405, 1987.
[5] J. A. Zeni, Jr., and J. S. Higginson, "Gait parameters and stride-to-stride variability during familiarization to walking on a split-belt treadmill," *Clin. Biomech.*, vol. 25, no. 4, pp. 383–386, 2010.
[6] D. S. Reisman, R. Wityk, K. Silver, and A. J. Bastian, "Locomotor adaptation on a split-belt treadmill can improve walking symmetry post-stroke," *Brain*, vol. 130, no. 7, pp. 1861–1872, 2007.
[7] T. J. W. Buurke, C. J. C. Lamoth, D. Vervoort, L. H. V. van der Woude, and R. den Otter, "Adaptive control of dynamic balance in human gait on a split-belt treadmill," *J. Exp. Biol.*, vol. 221, no. 13, 2018, Art. no. jeb174896.
[8] J. A. Roper, R. T. Roemmich, M. D. Tillman, M. J. Terza, and C. J. Hass, "Split-belt treadmill walking alters lower extremity frontal plane mechanics," *Eur. J. Appl. Physiol.*, vol. 33, no. 3, pp. 256–260, 2017.
[9] L. H. Sloot, M. M. van der Krogt, and J. Harlaar, "Self-paced versus fixed speed treadmill walking," *Gait Posture*, vol. 39, no. 1, pp. 478–484, 2014.
[10] A. Vazquez, M. A. Statton, S. A. Busgang, and A. J. Bastian, "Split-belt walking adaptation recalibrates sensorimotor estimates of leg speed but not position or force," *J. Neurophysiol.*, vol. 114, no. 6, pp. 3255–3267, 2015.
[11] A. Frigon, Y. Thibaudier, and M.-F. Hurteau, "Modulation of forelimb and hindlimb muscle activity during quadrupedal tied-belt and split-belt locomotion in intact cats," *Neuroscience*, vol. 290, pp. 266–278, Apr. 2015.
[12] A. Frigon, M.-F. Hurteau, Y. Thibaudier, H. Leblond, A. Telonio, and G. D'Angelo, "Split-belt walking alters the relationship between locomotor phases and cycle duration across speeds in intact and chronic spinalized adult cats," *J. Neurosci.*, vol. 33, no. 19, pp. 8559–8566, 2013.
[13] T. Ogawa, N. Kawashima, T. Ogata, and K. Nakazawa, "Predictive control of ankle stiffness at heel contact is a key element of locomotor adaptation during split-belt treadmill walking in humans," *J. Neurophysiol.*, vol. 111, no. 4, pp. 722–732, 2014.
[14] S. Fujiki, S. Aoi, T. Funato, N. Tomita, K. Senda, and K. Tsuchiya, "Adaptation mechanism of interlimb coordination in human split-belt treadmill walking through learning of foot contact timing: A robotics study," *J. Roy. Soc. Interface*, vol. 12, no. 110, 2015, Art. no. 20150542.
[15] D. S. Reisman, A. J. Bastian, and S. M. Morton, "Neurophysiologic and rehabilitation insights from the split-belt and other locomotor adaptation paradigms," *Phys. Therapy*, vol. 90, no. 2, pp. 187–195, 2010.
[16] S. A. Kautz, M. G. Bowden, D. J. Clark, and R. R. Neptune, "Comparison of motor control deficits during treadmill and overground walking poststroke," *Neurorehabilitation Neural Repair*, vol. 25, no. 8, pp. 756–765, 2011.
[17] W. Nanhoe-Mahabier, A. H. Snijders, A. Delval, V. Weerdesteyn, J. Duysens, S. Overeem, and B. R. Bloem "Split-belt locomotion in Parkinson's disease with and without freezing of gait," *Neuroscience*, vol. 236, pp. 110–116, Apr. 2013.
[18] S. Lauzière, C. Miéville, C. Duclos, R. Aissaoui, and S. Nadeau, "Perception threshold of locomotor symmetry while walking on a split-belt treadmill in healthy elderly individuals," *Perceptual Motor Skills*, vol. 118, no. 2, pp. 475–490, 2014.

[19] M. Betschart, B. J. McFadyen, and S. Nadeau, "Repeated split-belt treadmill walking improved gait ability in individuals with chronic stroke: A pilot study," *Physiotherapy Theory Pract.*, vol. 34, no. 2, pp. 81–90, 2018.
[20] J. Seuthe *et al.*, "Split-belt treadmill walking in patients with Parkinson's disease: A systematic review," *Gait Posture*, vol. 69, pp. 187–194, Mar. 2019.
[21] J. Feasel, M. C. Whitton, L. Kassler, F. P. Brooks, and M. D. Lewek, "The integrated virtual environment rehabilitation treadmill system," *IEEE Trans. Neural Syst. Rehabil. Eng.*, vol. 19, no. 3, pp. 290–297, Jun. 2011.
[22] G. Jayaram, B. Tang, R. Pallegadda, E. V. L. Vasudevan, P. Celnik, and A. Bastian, "Modulating locomotor adaptation with cerebellar stimulation," *J. Neurophysiol.*, vol. 107, no. 11, pp. 2950–2957, 2012.
[23] D. S. Reisman, H. J. Block, and A. J. Bastian, "Interlimb coordination during locomotion: What can be adapted and stored?" *J. Neurophysiol.*, vol. 94, no. 4, pp. 2403–2415, 2005.
[24] R. E. Fellin, W. C. Rose, T. D. Royer, and I. S. Davis, "Comparison of methods for kinematic identification of footstrike and toe-off during overground and treadmill running," *J. Sci. Med. Sport*, vol. 13, no. 6, pp. 646–650, 2010.
[25] L. Smith, S. Preece, D. Mason, and C. Bramah, "A comparison of kinematic algorithms to estimate gait events during overground running," *Gait Posture*, vol. 41, no. 1, pp. 39–43, 2015.
[26] J. M. Jasiewicz, J. H. Allum, J. W. Middleton, A. Barriskill, P. Condie, B. Purcell, and R. C. Li, "Gait event detection using linear accelerometers or angular velocity transducers in able-bodied and spinal-cord injured individuals," *Gait Posture*, vol. 24, no. 4, pp. 502–509, 2006.
[27] P. C. Formento, R. Acevedo, S. Ghoussayni, and D. Ewins, "Gait event detection during stair walking using a rate gyroscope," *Sensors*, vol. 14, no. 3, pp. 5470–5485, 2014.
[28] Y. Moon, R. S. McGinnis, K. Seagers, R. W. Motl, N. Sheth, J. A. Wright, Jr., R. Ghaffari, and J. J. Sosnoff, "Monitoring gait in multiple sclerosis with novel wearable motion sensors," *PLoS ONE*, vol. 12, no. 2, 2017, Art. no. e0171346.
[29] A. Muro-De-La-Herran, B. Garcia-Zapirain, and A. Mendez-Zorrilla, "Gait analysis methods: An overview of wearable and non-wearable systems, highlighting clinical applications," *Sensors*, vol. 14, no. 2, pp. 3362–3394, 2014.
[30] A. Hreljac and R. N. Marshall, "Algorithms to determine event timing during normal walking using kinematic data," *J. Biomech.*, vol. 33, no. 6, pp. 783–786, 2000.
[31] C. M. O'Connor, S. K. Thorpe, M. J. O'Malley, and C. L. Vaughan, "Automatic detection of gait events using kinematic data," *Gait Posture*, vol. 25, no. 3, pp. 469–474, Mar. 2007.
[32] A. R. Altman, D. S. Reisman, J. S. Higginson, and I. S. Davis, "Kinematic comparison of split-belt and single-belt treadmill walking and the effects of accommodation," *Gait Posture*, vol. 35, no. 2, pp. 287–291, 2012.
[33] E. V. L. Vasudevan, R. J. Hamzey, and E. M. Kirk, "Using a split-belt treadmill to evaluate generalization of human locomotor adaptation," *J. Visualized Exp.*, vol. 126, p. e55424, Aug. 2017.
[34] R. M. Kiss, "Comparison between kinematic and ground reaction force techniques for determining gait events during treadmill walking at different walking speeds," *Med. Eng. Phys.*, vol. 32, no. 6, pp. 662–667, 2010.
[35] S. Mo and D. H. K. Chow, "Accuracy of three methods in gait event detection during overground running," *Gait Posture*, vol. 59, pp. 93–98, Jan. 2018.
[36] M. P. Kadaba, H. K. Ramakrishnan, M. E. Wootten, J. Gainey, G. Gorton, and G. V. Cochran, "Repeatability of kinematic, kinetic, and electromyographic data in normal adult gait," *J. Orthopaedic Res.*, vol. 7, no. 6, pp. 849–860, 1989.
[37] S. Balasubramanian, A. Melendez-Calderon, A. Roby-Brami, and E. Burdet, "On the analysis of movement smoothness," *J. Neuroeng. Rehabil.*, vol. 12, no. 1, p. 112, 2015.
[38] J. A. Zeni, J. G. Richards, and J. S. Higginson, "Two simple methods for determining gait events during treadmill and overground walking using kinematic data," *Gait Posture*, vol. 27, no. 4, pp. 710–714, 2008.
[39] T. Fawcett, "An introduction to ROC analysis," *Pattern Recognit. Lett.*, vol. 27, no. 8, pp. 861–874, Jun. 2006.
[40] W. J. Youden, "Index for rating diagnostic tests," *Cancer*, vol. 3, no. 1, pp. 32–35, 1950.
[41] D. A. Bruening and S. T. Ridge, "Automated event detection algorithms in pathological gait," *Gait Posture*, vol. 39, no. 1, pp. 472–477, 2014.
[42] N. Fusco and A. Crétual, "Instantaneous treadmill speed determination using subject's kinematic data," *Gait Posture*, vol. 28, no. 4, pp. 663–667, 2008.

USMAN RASHID received the B.Sc. degree in electrical engineering from the University of Engineering and Technology, Taxila, in 2011, the M.S. degree in robotics and intelligent machines engineering from the National University of Sciences and Technology, Islamabad, in 2015. He is currently pursuing the Ph.D. degree with the Auckland University of Technology, Auckland.

His research interests include control systems, artificial intelligence, brain–computer interfaces, and inferential statistics.

NITIKA KUMARI received the bachelor's degree in physiotherapy, in 2010 and the master's degree in physiotherapy (rehabilitation), in 2013. She is currently pursuing the Ph.D. degree with the Auckland University of Technology (AUT), Auckland.

She has been a full-time Physiotherapist in India for two years, where she has been involved in neurology, community-based rehabilitation, musculoskeletal, and cardio-pulmonary conditions. Her research interests include stroke rehabilitation and the use of neuromodulatory interventions to facilitate motor learning.

DENISE TAYLOR received the Graduate Diploma degree in physiotherapy from Coventry University, Coventry, in 1986, the M.Sc. degree in rehabilitation from Southampton University, Southampton, in 1991, and the Ph.D. degree from the University of Otago, Dunedin, in 2004. Her Ph.D. research was focused on motor control.

She is currently a Professor with the School of Clinical Sciences, Auckland University of Technology, Auckland. Her research interests include neurological rehabilitation and health of older adults. Recently, she has been involved in research and implementation work based on the ideas of population health to improve the health of large populations of people rather than focusing on change at an individual level. This is a different approach in physiotherapy, which mainly focuses on treatment at an individual level. As part of this work, she has become increasingly aware of the importance of economic evaluations alongside clinical trials. In a recently completed multi-site randomized controlled trial of falls prevention in older adults, she was involved in conducting an economic evaluation. Working alongside an economist on this trial sparked her interest and she went on to study health economics, from 2009 to 2010 at the University of Aberdeen and have attended a course on Advanced Methods of Cost-Effectiveness Analysis, in 2011, run by the Health Economics Research Centre, University of Oxford. In 2012, she attended a workshop on Discrete Choice Experiments, run by the Health Economics Research Centre, Aberdeen. This is a relatively new method of health economic evaluation that could be particularly pertinent for rehabilitation research.

TIM DAVID received the B.S. and Ph.D. degrees from the University of Leeds, Leeds.

He is currently a Professor with the Department of Mechanical Engineering, University of Canterbury, Christchurch. His research interests include neurovascular coupling, dynamics of large vascular trees, mathematical and numerical models of cardiovascular blood flow, computational physiology, and dynamics of coupled cells.

Dr. David is a member of many professional organizations, including the Institute of Physics and Engineering in Medicine (IPEM), the Institution of Professional Engineers New Zealand (IPENZ), the Royal Society of New Zealand (RSNZ), and the Institute of Mathematics and its Applications.

NADA SIGNAL'S Ph.D. explored locomotor rehabilitation for people with stroke.

She trained as a Physiotherapist and has extensive clinical and managerial experience in the rehabilitation sector. She was involved in rehabilitation research since embarking on her M.HSc. degree, in 2003. Her research focuses on novel and theoretically sound rehabilitation interventions, including rehabilitation technologies. She is currently a Senior Research Fellow with the Health and Rehabilitation Research Institute, Auckland University of Technology. She is interested how knowledge of the underlying mechanisms associated with impairments, activity limitations, and participatory restrictions may inform the development and implementation of rehabilitation technologies.